Microchimica Acta (2019) 186: 144
https://doi.org/10.1007/s00604-019-3257-4

ORIGINAL PAPER

Uniform arrangement of gold nanoparticles on magnetic core particles with a metal-organic framework shell as a substrate for sensitive and reproducible SERS based assays: Application to the quantitation of Malachite Green and thiram

Huasheng Lai[1] · Wenjuan Shang[1] · Yuyin Yun[1] · Danjiao Chen[1] · Liqian Wu[1] · Fugang Xu[1]

Received: 22 October 2018 / Accepted: 16 January 2019 / Published online: 1 February 2019

Abstract

Magnetite (Fe_3O_4) spheres acting as a core were evenly decorated with gold nanoparticles (AuNPs) and coated with a shell of a metal organic framework (MOF) of type MIL-100(Fe). The resulting hybrid nanomaterial of type Fe_3O_4-Au@MIL-100(Fe) hybrid is shown to be a viable new SERS substrate. The integration of magnetic core, build-in plasmonic gold nanoparticles and a MOF shell endows the Fe_3O_4-Au@MIL-100(Fe) with highly efficient magnetic separation and enrichment ability, abundant interparticle hotspots, and significant chemical enhancement effect. This leads to a large enhancement, and greatly improved reproducibility of the SERS signals as shown for Malachite Green (MG) and the fungicide thiram. MG in solution can be quantified with a 50-fold lower detection limit (0.14 nM for peak at 1398 cm^{-1}) and largely improved reproducibility (RSD = 9%, 1398 cm^{-1}) when compared to the use of (a) AuNPs anchored on MIL-100(Fe) (RSD = 27%, 1186 cm^{-1}), or (b) AuNPs embedded in MIL-100(Fe) (RSD = 36%, 1398 cm^{-1}). The method was applied to the quantitation of MG and thiram in spiked water samples. The lower limits of detection are 4.4 nM for MG (1398 cm^{-1}) and 15 nM for thiram (1380 cm^{-1}), respectively, and signals' RSDs are 13% (1398 cm^{-1}) and 5% (1380 cm^{-1}) for MG and thiram, respectively. The substrate is recyclable.

Keywords Metal organic framework (MOF) · Surface enhanced Raman scattering (SERS) · Enhancement substrate · Plasmonic nanoparticles · Magnetic material · Multifunctional hybrid

Introduction

Surface-enhanced Raman scattering (SERS) is a powerful analytical tool with promising applications in various fields [1–4]. To achieve these promising application, it is essential to develop a reliable SERS substrates with high enhancement ability, good signal reproducibility and well stability. Compared with traditional single component Au/Ag nanostructured substrates [5–7], more explorations have turned to fabricate multicomponent hybrid substrates [8–10]. By integrating Au/Ag nanoparticles with other functional materials, hybrid SERS substrates not only display high sensitivity, good reproducibility and stability, but also show attractive and versatile properties (such as reusability, magnetic susceptibility, extraction ability, flexibility) for practical applications [11, 12], largely extending the application area of SERS. Considering this, integrating new functional materials with plasmonic particles in a rational design to fabricate efficient hybrid substrates is still in great demand to advance the application of SERS.

Metal-organic frameworks (MOFs) [13, 14] have received considerable attentions as scaffold or substrate for SERS analysis [15–23]. For example, Sada demonstrated earliest the SERS sensing application of AuNRs in MOF [15, 16]; Yu first reported the direct observation of SERS effect on MOF surface [17]; Van Duyne employed a MOF film over AgFON as capture layer to detect volatile organic compounds (VOC) that do not adsorb on conventional Au/Ag substrate [18]. After that, various structured hybrid including AuNPs embedded in MOF [19, 20], AgNPs anchored on MOF [21, 22], core-shell type AuNPs@MIL-

Electronic supplementary material The online version of this article (https://doi.org/10.1007/s00604-019-3257-4) contains supplementary material, which is available to authorized users.

✉ Fugang Xu
fgxu@jxnu.edu.cn

Huasheng Lai
Laihs@foxmail.com

[1] College of Chemistry and Chemical Engineering, Jiangxi Normal University, Nanchang 330022, People's Republic of China

100(Fe) [23] were reported for sensitive SERS detection of important biomolecules or toxic analytes. These explorations clearly demonstrate that MOFs with chemical enhancement effect, large surface area, strong absorption, uniform pores have great potential in constructing highly efficient SERS substrate. However, the challenges are also obvious for application of MOF-plasmonic hybrid in SERS: (i) it is of great importance and urgent to improve the reproducibility of the SERS signal obtained on MOF-plasmonic hybrids. For Au/Ag embedded in or anchored on MOFs, the Au/Ag particle's shape, size and distribution are hard to control, leading to poor signal reproducibility; (ii) it is hard to form efficient hot-spots for single particle Au/Ag core-MOF shell hybrid, resulting in low enhancement; (iii) roles of MOFs are usually limited to supporting matrix or adsorption enhancer and (iv) the substrate is simple in function, leading to a low detection sensitivity and tedious operation (such as repeated centrifugation) for sample detection. As the research on MOFs in SERS analysis is still in its infancy, new explorations are in great demand to develop novel structured plasmonic particle-MOF hybrid for simple, sensitive and reproducible SERS analysis.

Herein, a sandwich-structured hybrid composed of Fe_3O_4 core-Au NPs interlayer-MIL-100(Fe) shell [Fe_3O_4-Au@MIL-100(Fe)] (Scheme 1) was developed as a SERS substrate for reproducible and sensitive molecule sensing. Fe_3O_4 as core plays important role in uniformly and densely loading Au NPs in a relatively controlled manner, guaranteeing the reproducibility of the SERS signal. Besides, it also brings facile operation and concentration effect. Compared with other similar NPs-MOFs or conventional Au/Ag substrates, the Fe_3O_4-Au@MIL-100(Fe) hybrid have enormous advantages due to its multifunction-characteristic: (i) fast separation and easy operation during preparation and detection procedure; (ii) great improved reproducibility due to uniform distribution of AuNPs; (iii) significant chemical enhancement ability from MOF shells; (iv) giant enhancement ability due to the combination of magnetic concentration, electromagnetic enhancement of AuNPs and chemical enhancement of MOF. The hybrid substrate was used to quantitative detection of MG and thiram in standard solution and lake water sample, which showed good regression coefficient ($R^2 > 0.99$), low LOD (4.4 nM for MG, 15 nM for thiram) and excellent signal reproducibility (RSD was less than 13% for MG detection, or 6% for thiram detection). Importantly, the reproducibility was greatly improved compared with those of AuNPs embedded in MOF-100(Fe) or AuNPs loaded on MOF-100(Fe). Besides, good recyclability was also observed on this Fe_3O_4-Au@MIL-100(Fe) hybrid substrate for dye detection. Such a robust Fe_3O_4-Au@MIL-100(Fe) hybrid as a efficient SERS-active substrate possesses great potential in environment monitoring.

Experimental section

Materials and reagents

Chloroauric acid ($HAuCl_4$), Malachite Green (MG), thiram, 1,3,5-tricarboxybenzene (BTC), and polyvinylpyrrolidone (PVP, K30) were purchased from Sinopharm Chemical Reagent Co., Ltd., China (https://www.sinoreagent.com). Ferric chloride (anhydrous) ($FeCl_3$), trisodium citrate dihydrate (Na_3Cit), sodium acetate anhydrous (NaAc), ethylene glycol (EG), poly(methacrylic acid, sodium salt) (PMAA; average $M_w = 9500$), branched poly(ethyleneimine) (BPEI; average $M_w = 25{,}000$) were purchased from Aladdin Reagent Co., Ltd. (Shanghai, China, http://www.aladdin-e.com). All reagents were used without further purification. Deionized water (resistancy >18.2 MΩ·cm) was purified by using a MilliQ system.

Fabrication of Fe_3O_4-Au@MIL-100(Fe)

The magnetite particles were synthesized according to a solvothermal method [24] and our previous work [25]. Then Fe_3O_4-gold nanoparticles was prepared by Zhai's method [26]. Finally, coating of the Fe_3O_4-Au with MIL-100(Fe) was performed according to a reported approach with some modification [23]. Details of these preparation can be found in the electronic supplementary material.

Characterization methods

Scanning electron microscopy (SEM) imagines and energy dispersive X-ray analyzer were acquired on a S3400 N SEM

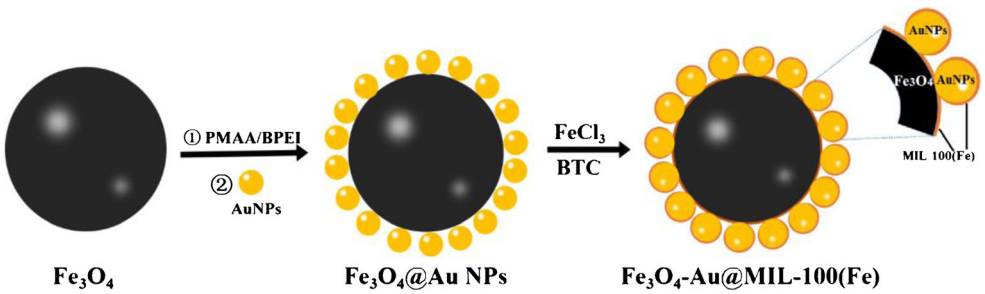

Scheme 1 Schematic illustration of the preparation procedure of Fe_3O_4-Au@MIL-100(Fe). PMMA: poly(methacrylic acid; BPEI: branched poly(ethyleneimine); BTC: 1,3,5-tricarboxybenzene

equipped with a Phoenix energy dispersive X-ray analyzer (EDXA) (Hitachi, Japan, https://www.hitachi-hightech.com). Transmission electron microscopy (TEM) images were obtained via a JEM-2100F TEM (JEOL Ltd., https://www.jeol.co.jp). The absorption spectra were measured using a U-3900H UV-vis spectrophotometer (Hitachi, Japan, https://www.hitachi-hightech.com). All the Raman spectra measurements were performed on a LabRAM-HR Raman system (Horiba, Japan, http://www.horiba.com) with a He-Ne laser resource. The excitation wavelength was 633 nm, and the laser power was about 1 mW with an integration time of 5 s. For each spectrum, the average of at least five measurements was presented.

SERS measurements

The stock solution of MG (10^{-4} M) was prepared in ethanol. Then MG solutions with the concentration from 10^{-5} M to 10^{-9} M were prepared by the step-by-step dilution of 1 mL the stock solution with 9 mL water. The stock solution of thiram (2 mM) was prepared in methanol and then diluted into different concentrations by water.

For SERS measurement, 20 μL of the hybrids suspension (10 mg·mL^{-1}) was mixed with 20 μL MG solution and incubated for 1 h. After that, the mixture solution was collected by a magnet and dropped on the clean silicon wafer carefully, dried in ambience for SERS measurements.

For real sample analysis, local lake water was collected and certain concentration of dye was added. The solution was filtered through a 0.2 mm PTFE filter, and the filtrate was collected. Then, 20 μL of the filtrate was mixed with 20 μL hybrid substrate suspension followed by incubation, separation and detection operation as the same for standard solution analysis. The average results from 5 measurements were presented. And the SERS signal of MG at 1398 cm^{-1} and thiram at1380 cm^{-1} was used for quantification.

Recycle test of the Fe_3O_4-Au@MIL-100(Fe)

After the SERS signal was recorded for the first time as mentioned above, the substrate was detached from the silicon wafer by ultrasonic treatment and then ultrasonically washed (10 s per time and repeat 3 times) in 4 mL ethanol solution, and the volume of the Fe_3O_4-Au@MIL-100(Fe) ethanol solution was fixed to 1 ml. The washed Fe_3O_4-Au@MIL-100 (Fe) was again mixed with 10^{-5} M MG solution with equal volume for next detection to obtain the SERS signal for the second time. This detection-washing procedure was repeated to test the recyclability of the Fe_3O_4-Au@MIL-100 (Fe) substrate.

Results and discussions

Characterization of the Fe_3O_4-Au@MIL-100 (Fe)

The preparation of MNPs-Au@MIL-100(Fe) is showed in Scheme 1, and detailed procedure can be found in the supporting information.

The morphology of the products was characterized by SEM and TEM. Figure 1 shows Fe_3O_4 spheres with diameter of about 320 ± 34 nm (n = 100) are successfully prepared. Figure 1-b and c display a considerable number of Au NPs with a narrow size distribution of 15 ± 3 nm (n = 100) are evenly attached onto Fe_3O_4 sphere to form MNPs-AuNPs composite. For MNPs-Au@MIL-100(Fe), Fig. 1-d shows a light-grey layer with thickness of about 2 ± 1 nm (n = 50) covered around Au NPs or the whole Fe_3O_4-Au composite, indicating the formation of MOF shell. It is noticeable that the inner Au NPs decorated on Fe_3O_4 sphere do not show obvious change in morphology (no obvious aggregation or detachment) after MOF shell coating. Thus a high and homogeneous enhancement ability is guaranteed.

For comparison, two typical previously reported plasmonic particle-MOF hybrid structures including AuNPs anchored on MIL-100(Fe) and AuNPs embedded in MOF-100(Fe) were also prepared. For AuNPs anchored on MOF-100(Fe), the distribution of AuNPs is quite uneven (Fig. S1-a) as either sparseness or aggregation can be observed. For Au NPs embedded in MIL-100(Fe) (Fig.S1-b), only few numbers of Au NPs are embedded in MIL-100(Fe) and their distribution are random. These uncontrollable and inhomogeneous distribution of Au NPs can cause poor signal reproducibility (as discussed in the following section) and greatly hinder its practical sensing application. Through comparison, it is obvious that the proposed approach, which introducing Fe_3O_4 as core and using electrostatic assembly to prepare plasmonic particle-MOF hybrid, is more controllable, and the obtained Fe_3O_4-Au@MIL-100(Fe) substrate should have great potential for highly sensitive and reproducible SERS analysis.

The crystal structures of the composites were characterized by XRD and the results are shown in Fig. 2. The XRD spectrum of Fe_3O_4 displays diffraction peaks with 2θ at 18.3°, 30.3°, 35.6°, 43.3°, 53.6°, 57.4° and 62.9°, corresponded to the (1 1 1), (2 2 0), (3 1 1), (4 0 0), (4 2 2), (5 1 1) and (4 4 0) planes of pure cubic spine crystal structure of magnetite Fe_3O_4, respectively (JCPDS No. 19–0629). Compared with Fe_3O_4, several new peaks at 2θ of 38.2°, 44.3°, 64.6°, 77.6° and 81.7° appear in Fe_3O_4-Au. These peaks corresponding to the (1 1 1), (2 0 0), (2 2 0), (3 1 1), and (2 2 2) plane of face-centered cubic phase of gold (JCPDS No. 04–0784), implying the successful adsorption of AuNPs on Fe_3O_4 sphere. For MIL-100(Fe) encapsulated Fe_3O_4-Au, the diffraction peaks are well matched with that of Fe_3O_4-Au, and an additional diffraction peak at 2θ around 10° is corresponding to the (4

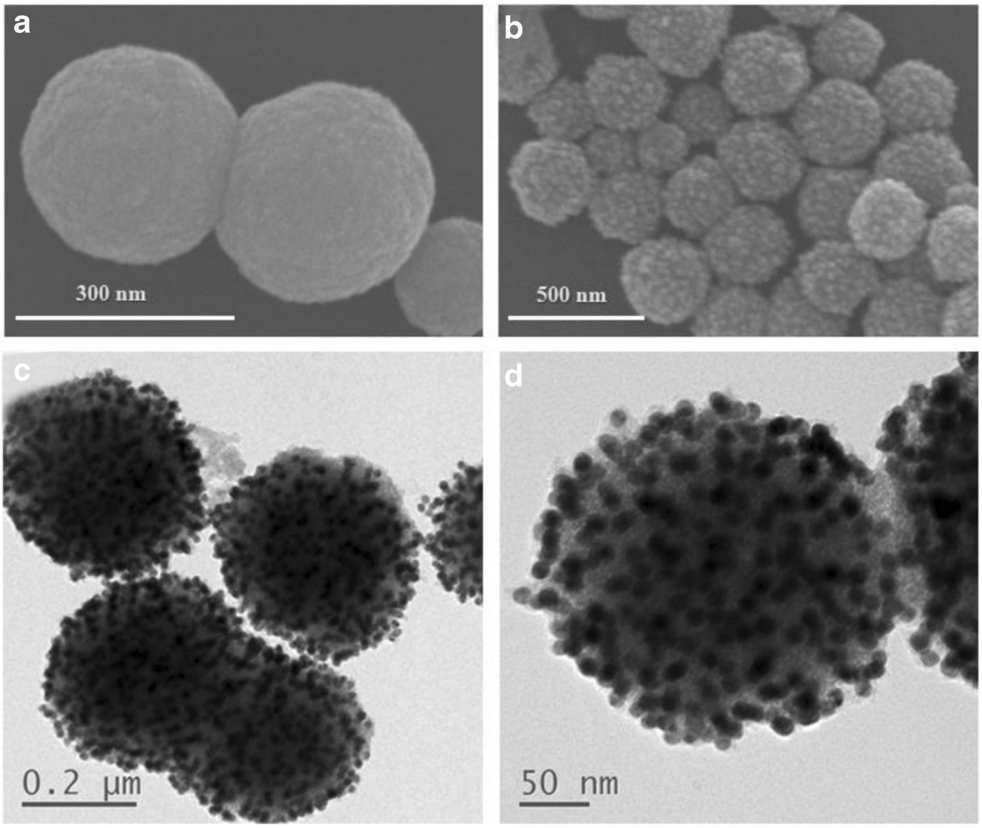

Fig. 1 SEM image of (**a**) Fe_3O_4, (**b**) Fe_3O_4-Au, (**c**) and (d) TEM image of Fe_3O_4-Au@MIL-100(Fe) in different image resolution

2 8) plane [27], which indicating MIL-100(Fe) is grew onto Fe_3O_4-Au. The weak peak intensity of MIL-100(Fe) may be due to its thin thickness. However, the following results indicate even such thin MOF shell plays considerable role in amplify the SERS signal.

According to the results from SEM, TEM, XRD, and VSM and UV-via spectroscopy in ESM, we can conclude that the Fe_3O_4-Au@MIL-100(Fe) hybrids with magnetic sphere as core, uniform distributed Au nanoparticles as interlayer and a thin MIL-100 as coating are successfully fabricated.

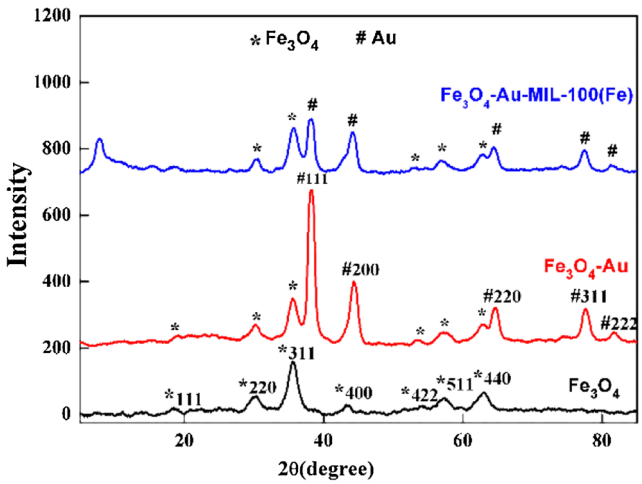

Fig. 2 XRD pattern of Fe_3O_4, Fe_3O_4-Au, and Fe_3O_4-Au@MIL-100(Fe)

SERS activity of Fe_3O_4-Au@MIL-100(Fe)

Our study is devoted to fabricating a highly efficient, multifunctional SERS-active substrate. It is expected the Fe_3O_4-Au@MIL-100(Fe) should be very attractive in SERS analysis as the hybrid integrated magnetic core with fast separation and concentration ability, build-in plasmonic nanoparticles with the localized surface plasmon resonance property, and the MIL-100(Fe) shell with high adsorption capability as reported all-in-one. However, the enhancement of shell isolated nanoparticles deceases rapidly with the increase of shell thickness [28]. Therefore, Fe_3O_4-Au@MIL-100(Fe) hybrids with MIL-100(Fe) shell formed by one assembly cycle are used to test SERS performance. Aromatic dye malachite green (MG) is used as a probe. The SERS responses of various substrates are presented in Fig. 3a. It can be seen no SERS signals of MG can be found when Fe_3O_4 sphere is used as substrate (black line in Fig. 3a). For Fe_3O_4-Au, obvious characteristic Raman peaks of MG is presented. The Raman peaks of MG at 445 cm^{-1}, 1180 cm^{-1}, 1370 cm^{-1} and 1618 cm^{-1} are generated from out of-plane modes of phenyl-C-phenyl, in-plane modes of C-H bending, N-phenyl stretching, and ring C-C stretching, respectively. The medium bands at 916 cm^{-1},

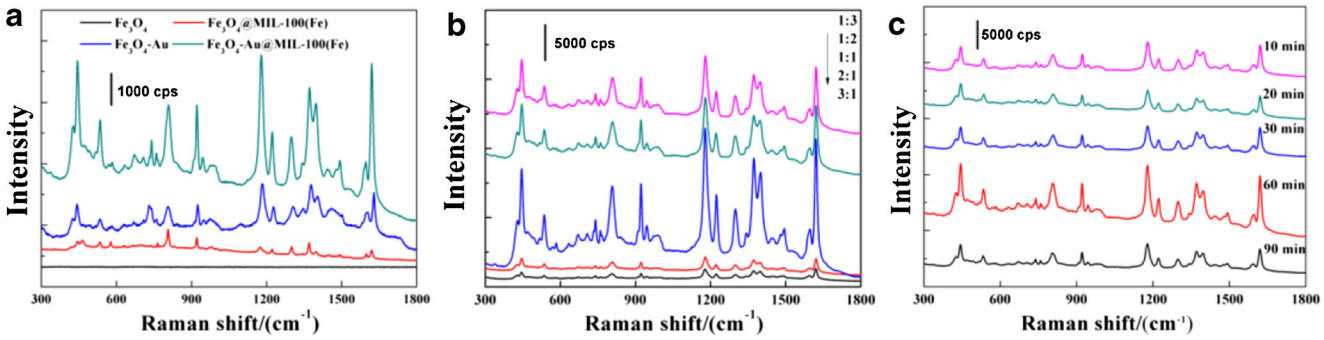

Fig. 3 **a** SERS spectrum of MG obtained from different substrate: from bottom to top is Fe_3O_4, Fe_3O_4@MIL-100(Fe), Fe_3O_4-Au, and Fe_3O_4-Au@MIL-100(Fe), respectively. SERS spectrum of MG with Fe_3O_4-Au@MIL-100(Fe), **b** with different volume ratio of (Fe_3O_4-Au@MIL-100(Fe) versus MG) from 1:3 to 3:1; **c** with different mixture time of 10 min, 20 min, 30 min, 60 min, 90 min

1220 cm^{-1} and 1398 cm^{-1} are caused by C-H out-of-plane bending, C-H rocking and N-phenyl stretching [29]. This indicating that AuNPs play a vital role in amplifying the SERS signal of MG. An interesting result is observed for Fe_3O_4@MIL-100(Fe). The red curve in Fig. 3a shows clear Raman peaks of MG are obtained on Fe_3O_4@MIL-100(Fe), and the Raman intensity is only a little weaker than that obtained on Fe_3O_4-Au. As the Fe_3O_4 does not show enhancement ability, thus, the enhancement can be ascribed to the MIL-100(Fe) shell as an enhancement membrane to amplify Raman intensities. This phenomenon is attributed to the strong π interaction between the benzene rings in MG and MIL-100(Fe) [30], and the enhancement is resulted from a possible chemical enhancement mechanism [17]. For Fe_3O_4-Au@MIL-100(Fe) (green curve) hybrid, the SERS signal of MG is much stronger than that of Fe_3O_4-Au (blue curve) and Fe_3O_4@MIL-100(Fe) (red curve). That is rational as the hybrid combines the electromagnetic enhancement of high-density Au nanoparticles decorated on Fe_3O_4 surface, and the chemical enhancement from MIL-100(Fe). The results indicate that a rational combination of functional material with plasmonic material brings about an additional amplification effect and greatly enhances the SERS signal.

Optimization of the SERS performance of Fe_3O_4-Au@MIL-100(Fe)

To investigate the optimized condition for sample analysis by this SERS substrate, the volume ratio and mixture time of Fe_3O_4-Au@MIL-100(Fe) solution and MG solution were studied. It can be seen in Fig. 3-b that the best Raman performance is exhibited when the volume ratio of Fe_3O_4-Au@MIL-100(Fe) solution to MG solution is 1:1. Moreover, the optimized mixture time test shows the strongest Raman intensity is obtaining when the sample is mixing with substrate for 60 min (Fig. 3-c). Hence, the following tests are performing by incubating equal volume of substrate Fe_3O_4-Au@MIL-100(Fe) and sample in a tube for 60 min before SERS analysis.

SERS detection of malachite green and thiram

For the SERS application of the multifunctional Fe_3O_4-Au@MIL-100(Fe) hybrids, malachite green (MG) and thiram are employed as sample molecules. MG, one of the toxic organic dyes, often is illegally added into aquaculture water as a bacteriostatic agent or an amoeba killing agent. Thiram, one of the typical dithiocarbamate fungicides, is widely used in agriculture, but extra uptake of thiram does great harm to human health. Thus, a sensitive method to detect these toxic molecules is of great importance.

The multifunctional SERS substrate Fe_3O_4-Au@MIL-100(Fe) is first used to detect MG in standard solution. As can be seen in Fig. 4-a, the characteristic peaks of MG at 445 cm^{-1}, 916 cm^{-1}, 1180 cm^{-1}, 1220 cm^{-1}, 1370 cm^{-1}, 1398 cm^{-1} and 1618 cm^{-1} can be observed clearly. As the concentration of MG decreases, the Raman intensities reduce rapidly. When the concentration is down to 10^{-9} M, several characteristic peaks of MG are still can be distinguished. The LOD of MG is about 1.4×10^{-10} M, which is about 50 times lower than that of AuNPs@MIL-100(Fe) (8×10^{-9} M) reported in ref. [23]. The comparison of the method and performance of different SERS substrates (materials) is also shown in Table S2. Moreover, the reproducibility of the signal obtained on Fe_3O_4-Au@MIL-100(Fe) is also investigated. As it can be seen in the Fig. 4-b, SERS spectrum of 10^{-5} M MG obtains in 10 random points shows good reproducibility, and the relative standard deviation (RSD) of Raman intensities of MG at 1180, 1398, 1618 cm^{-1} are 7.09%, 9.40%, 9.27%, respectively (Fig. 4-c). In contrast, the RSD of corresponding peaks are over 23% and 29% for AuNPs anchored on MIL-100(Fe) (Fig.S3-a) and AuNPs embedded in MIL-100(Fe) (Fig.S3-b), respectively, indicating a poor reproducibility. These high RSD are mainly due to the uneven distribution of AuNPs in these hybrids, which further conforming the advantages of the proposed approach in fabricating highly uniform and efficient SERS active hybrid. The greatly improved performance observed on Fe_3O_4-Au@MIL-100(Fe) can be ascribed to the contribution from following factors: Fe_3O_4

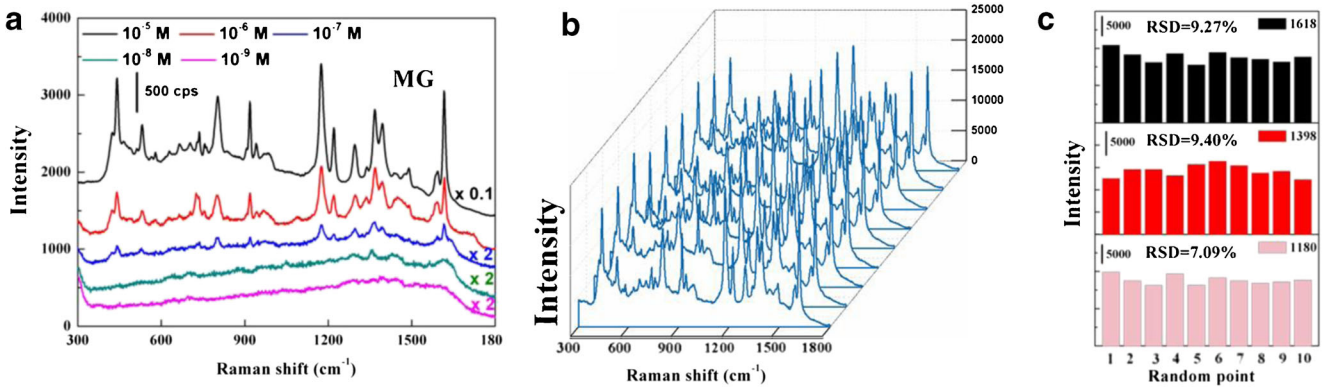

Fig. 4 SERS spectrum of MG (**a**) in different concentration of 10^{-5} - 10^{-9} M, (**b**) 10^{-5} M obtained in 10 random points; (**c**) corresponding RSD results of (**b**) calculated at 1180, 1398 and 1618 cm^{-1} Raman peaks

core concentrates the target and the substrate to form inter-sphere hot-spots; AuNPs assembly provides uniform and dense hot-spots; and MOF shell facilitates the adsorption of target and provides significant chemical enhancement. These factors work together and a synergy effect may happen, leading to greatly improved sensing performance.

For the real sample detection, local lake water was collected as environmental water sample, and then MG or thiram was spiked into it to test the SERS performance of the Fe_3O_4-Au@MIL-100(Fe) substrates for real sample analysis. MG spiked in the lake water still exhibits good SERS response in the range of 10^{-5} – 10^{-8} M (Fig. 5-a). A linear relationship is

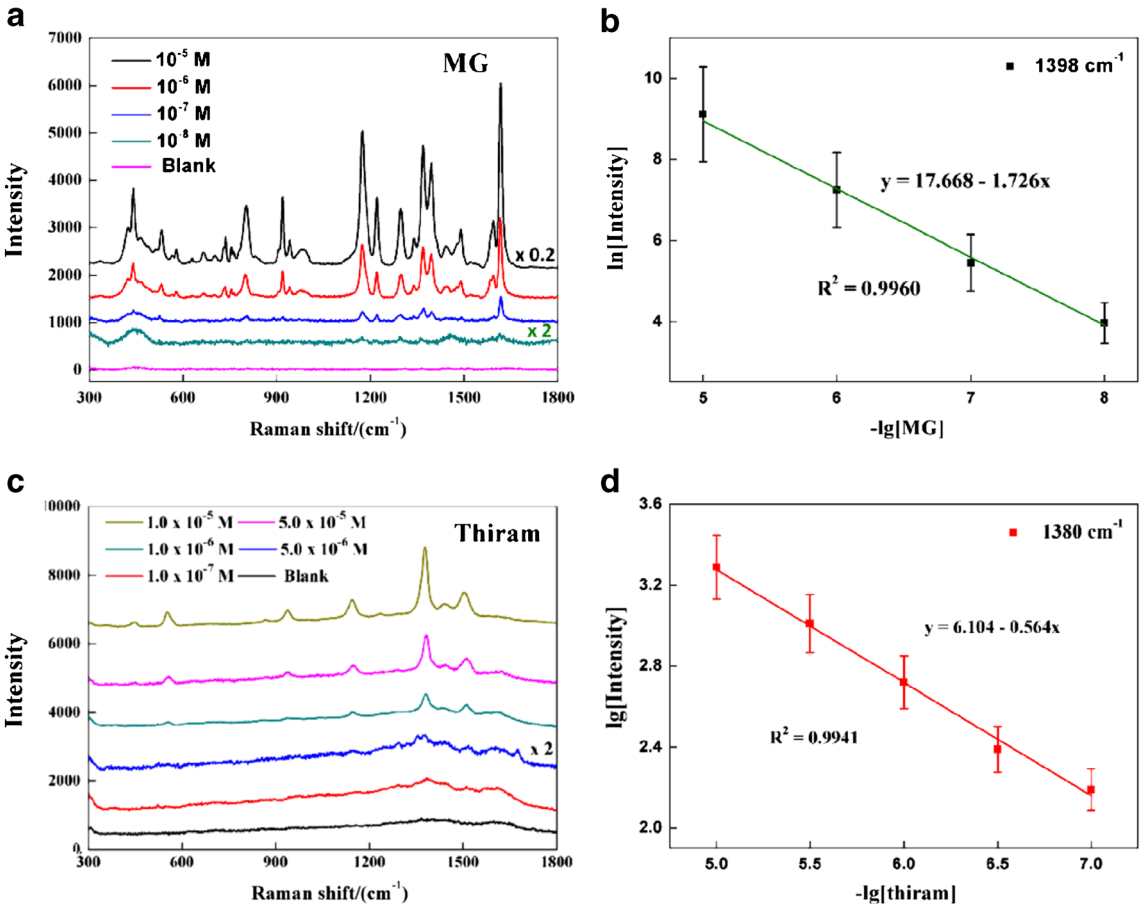

Fig. 5 SERS spectrum of different concentration of MG (**a**) and thiram (**c**) in lake water (after baseline and correction); (**b**) linear relationship of peak intensities at 1398 cm^{-1} versus natural logarithm [MG concentration] of (**a**); (**d**) linear relationship of peak intensities at 1380 cm^{-1} versus logarithm [thiram concentration] of (**c**)

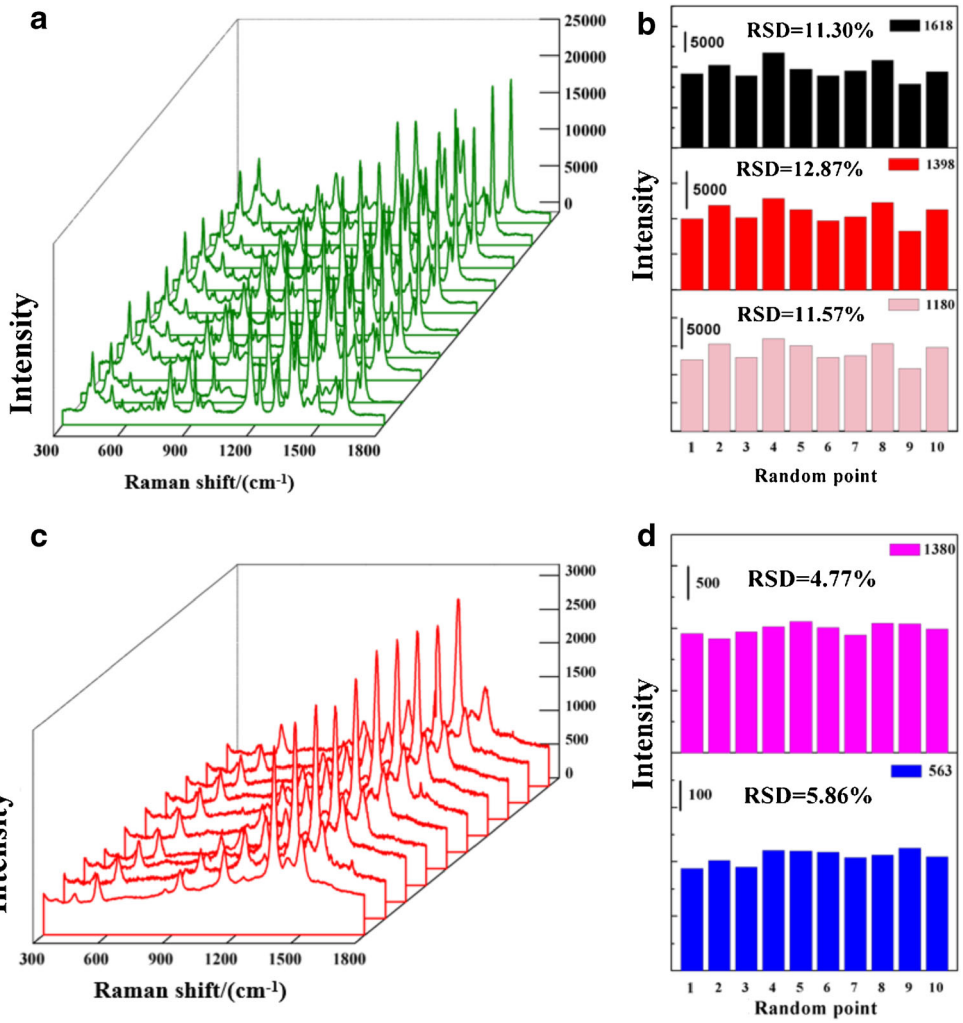

Fig. 6 SERS spectrum of 10^{-5} M MG (**a**) and thiram (**c**) in real water sample with Fe_3O_4-Au@MIL-100(Fe) obtained in 10 random points; (**b**) corresponding RSD results of (**a**) calculated at 1180, 1398 and 1618 cm^{-1} Raman peaks. (**d**) corresponding RSD results of (**c**) calculated at 563 and 1380 cm^{-1} Raman peaks

established between the Raman intensities at 1398 cm^{-1} and concentration of MG as y = 17.668–1.726x, and the corresponding correlation coefficient (R^2) is 0.9960 (Fig. 5-b).

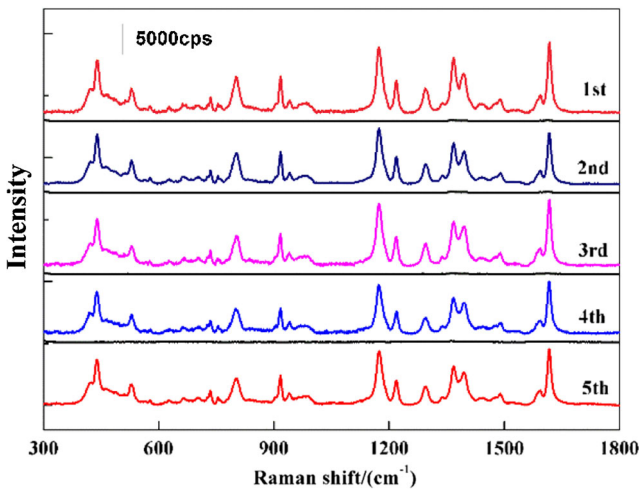

Fig. 7 SERS spectrum of 10^{-5} M MG with Fe_3O_4-Au@MIL-100(Fe) obtained during 1–5 detection-washing cycles

Take the background into consideration, the LOD of MG in real environmental water is about 4.4×10^{-9} M. On the other hand, the Raman intensities of thiram are shown in Fig. 5-c. The highest Raman intensity of thiram appeared at 1380 cm^{-1} is caused by the C-N stretching vibration and symmetric CH_3 deformation. Characteristic peak at 440 cm^{-1} is generated from CH_3NC deformation and C=S stretching vibration, 563 cm^{-1} is due to the stretching vibration of S=S, 925 cm^{-1} is originated from the stretching vibration of CH_3N and C=S. Moreover, CN stretching vibration and CH_3 rocking vibration result in the characteristic Raman peaks appeared at 1150 cm^{-1} and 1514 cm^{-1} [31]. Nonlinear relationships between Raman intensities of thiram at 563, 1380 cm^{-1} and the logarithm concentration of thiram in the range of 10^{-5} – 10^{-7} M are showed in Fig. 5-d. A linear relationship is establishing between SERS intensity at 1380 cm^{-1} and concentration of thiram as y = 6.104–0.564x, and R^2 = 0.9941 (Fig. 5-d). Based on this linear equation, the LOD of thiram is calculated as 1.5×10^{-8} M. Comparison of several SERS substrates for the detection of thiram is also showed in Table S2, which indicating that Fe_3O_4-Au@MIL-100(Fe) substrate exhibits

good sensitivity due to the synergy among component materials. Hence, the multifunctional Fe_3O_4-Au@MIL-100(Fe) can be used to detect trace toxic dye and pesticide residue for environmental analysis.

Besides a high sensitivity, the Fe_3O_4-Au@MIL-100(Fe) hybrid as SERS substrate also shows good reproducibility for real sample analysis. The reproducibility test is carried out at ten random sites for MG (Fig. 6-a) or thiram detection (Fig. 6-c). The relative standard deviation (RSD) of corresponding characteristic peaks of MG at 1180, 1398, 1618 cm^{-1} are 11.6%, 12.9%, 11.3%, respectively (Fig. 6-b), and RSD results of thiram at 1380 and 563 cm^{-1} are 4.8% and 5.9% (Fig. 6-d). These results implying that the Fe_3O_4-Au@MIL-100(Fe) composites substrates exhibit excellent reproducibility, which can be ascribed to the uniform distribution of AuNPs on the Fe_3O_4 core and the even coating of MIL-100(Fe) shell. Based on the excellent reproducibility and well-defined SERS intensity-analyte concentration dependence, reliable quantitative analysis can be achieved in applying the Fe_3O_4-Au@MIL-100(Fe) composites substrates for SERS detection application. Besides these molecules, the substrate also used to detect biomedically important dopamine, which also showed high sensitivity, indicating a great potential of the hybrid for SERS analysis.

The recyclability of the SERS substrate is an efficient way to reduce the cost of the substrate. Here, the recycle use of the Fe_3O_4-Au@MIL-100(Fe) is also investigated. Figure 7-a revealing that the Fe_3O_4-Au@MIL-100(Fe) substrate can be reused for 5 times without obvious attenuation of the Raman intensity, and the substrate shows no obvious signal after washing between each cycle.

Conclusions

A self-assembly strategy had been successfully used to fabricate a sandwich-structured Fe_3O_4-Au@MIL-100(Fe) hybrid as a multifunctional SERS substrate, which integrated fast separation and enrichment ability of Fe_3O_4 core, abundant and uniform hot spots of assembled AuNPs as interlayer, and significant chemical enhancement of MOF shell. The highly efficient substrate achieved quantitative analysis of MG and thiram in real water with good correlation coefficient, low LOD and excellent signal reproducibility. Besides, the substrate also displayed good recyclability. The proposed approach can be used to fabricate other multifunctional hybrid, and the prepared Fe_3O_4-Au@MIL-100(Fe) hybrid possesses great potential in environment monitoring.

Acknowledgements This work is financially supported by the National Natural Science Foundation of China (21705063, 21665011), Natural Science Foundation of Jiangxi Province (20161BAB203088).

Compliance with ethical standards The author(s) declare that they have no competing interests.

References

1. Schlücker S (2014) Surface-enhanced Raman spectroscopy: concepts and chemical applications. Angew Chem Int Edit 53:4756–4795
2. Ren X, Cheshari EC, Qi J, Li X (2018) Silver microspheres coated with a molecularly imprinted polymer as a SERS substrate for sensitive detection of bisphenol a. Microchim Acta 185(4):242
3. Li DW, Zhai WL, Li YT, Long YT (2014) Recent progress in surface enhanced Raman spectroscopy for the detection of environmental pollutants. Microchim Acta 181:23–43
4. Wang Z, Wu S, Ciacchi LC, Wei G (2018) Graphene-based nanoplatforms for surface-enhanced Raman scattering sensing. Analyst 143:5074–5089
5. Ding SY, You EM, Tian ZQ, Moskovits M (2017) Electromagnetic theories of surface-enhanced Raman spectroscopy. Chem Soc Rev 46:4042–4076
6. Nie S, Emory SR (1997) Probing single molecules and single nanoparticles by surface-enhanced Raman scattering. Science 275: 1102–1106
7. Wei G, Wang L, Sun LL, Song YH, Sun YJ, Guo CL, Yang T, Li Z (2007) Type I collagen-mediated synthesis and assembly of UV-photoreduced gold nanoparticles and their application in surface-enhanced Raman scattering. J Phys Chem C 111:1976–1982
8. Li X, Chen G, Yang L, Jin Z, Liu J (2010) Multifunctional au-coated TiO_2 nanotube arrays as recyclable SERS substrates for multifold organic pollutants detection. Adv Funct Mater 20:2815–2824
9. Zhang XQ, Zhu YH, Yang XL, Zhou Y, Yao YF, Li CZ (2014) Multifunctional Fe_3O_4@TiO_2@au magnetic microspheres as recyclable substrates for surface-enhanced Raman scattering. Nanoscale 6:5971–5979
10. Villa JEL, Santos DP, Poppi R (2016) Fabrication of gold nanoparticle-coated paper and its use as a sensitive substrate for quantitative SERS analysis. Microchim Acta 183:2745–2752
11. Qiu H, Wang M, Jiang S (2017) Reliable molecular trace-detection based on flexible SERS substrate of graphene/ag-nanoflowers/PMMA. Sensors Actuators B Chem 249:439–450
12. Lai HS, Xu FG, Wang L (2018) A review of the preparation and application of magnetic nanoparticles for surface-enhanced Raman scattering. J Mater Sci 53:8677–8698
13. Furukawa H, Cordova KE, O'Keeffe M, Yaghi OM (2013) The chemistry and applications of metal-organic frameworks. Science 44:1230444
14. Kreno LE, Leong K, Farha OK, Allendorf M, Van Duyne RP, Hupp JT (2012) Metal-organic framework materials as chemical sensors. Chem Rev 112:1105–1125
15. Sugikawa K, Furukawa Y, Sada K (2011) SERS-active metal-organic frameworks embedding gold nanorods. Chem Mater 23: 3132–3134
16. Sugikawa K, Nagata S, Furukawa Y, Kokado K, Sada K (2013) Stable and functional gold nanorod composites with a metal-organic framework crystalline shell. Chem Mater 25:2565–2570
17. Yu TH, Ho CH, Wu CY, Chien CH, Lin CH, Lee S (2013) Metal-organic frameworks: a novel SERS substrate. J Raman Spectrosc 44:1506–1511

18. Kreno LE, Greeneltch NG, Farha OK, Hupp JT, Van Duyne RP (2014) SERS of molecules that do not adsorb on ag surfaces: a metal-organic framework-based functionalization strategy. Analyst 139:4073–4080
19. Hu YL, Liao J, Wang DM, Li GK (2014) Fabrication of gold nanoparticle-embedded metal-organic framework for highly sensitive surface-enhanced Raman scattering detection. Anal Chem 86: 3955–3963
20. Cao X, Hong S, Jiang Z, She Y, Wang S, Zhang C, Li H, Jin F, Jin M, Wang J (2017) SERS-active metal-organic frameworks with embedded gold nanoparticles. Analyst 142:2640–2647
21. Jiang Z, Gao P, Yang L, Huang C, Li Y (2015) Facile in situ synthesis of silver nanoparticles on the surface of metal-organic framework for ultrasensitive surface-enhanced Raman scattering detection of dopamine. Anal Chem 87:12177–12182
22. Kuang X, Ye S, Li X, Ma Y, Zhang C, Tang B (2016) A new type of surface-enhanced Raman scattering sensor for the enantioselective recognition of D/L -cysteine and D/L -asparagine based on a helically arranged Ag NPs@homochiral MOF. Chem Commun 52: 5432–5435
23. Liao J, Wang DM, Liu AQ, Hu YL, Li GK (2015) Controlled stepwise-synthesis of core-shell au@MIL-100 (Fe) nanoparticles for sensitive surface-enhanced Raman scattering detection. Analyst 140:8165–8171
24. Liu J, Sun ZK, Deng YH, Zou Y, Li CY, Guo XH, Xiong LQ, Gao Y, Li FY, Zhao DY (2009) Highly water-dispersible biocompatible magnetite particles with low cytotoxicity stabilized by citrate groups. Angew Chem 121:5989–5993
25. Ding GH, Xie S, Zhu YM, Liu Y, Wang L, Xu FG (2015) Graphene oxide wrapped Fe_3O_4@au nanohybrid as SERS substrate for aromatic dye detection. Sensors Actuators B Chem 221:1084–1093
26. Zhai YM, Zhai JF, Wang YL, Guo SJ, Ren W, Dong SJ (2009) Fabrication of iron oxide core/gold shell submicrometer spheres with nanoscale surface roughness for efficient surface-enhanced Raman scattering. J Phys Chem C 113:7009–7014
27. Zhang HJ, Qi SD, Niu XY, Hu J, Ren CL (2014) Metallic nanoparticles immobilized in magnetic metal-organic frameworks: preparation and application as highly active, magnetically isolable and reusable catalysts. Catal Sci Technol 4:3013–3024
28. Li JF, Anema JR, Wandlowski T, Tian ZQ (2015) Dielectric shell isolated and graphene shell isolated nanoparticle enhanced Raman spectroscopies and their applications. Chem Soc Rev 44:8399–8409
29. Zhang Y, Huang Y, Zhai F, Du R, Liu Y, Lai K (2012) Analyses of enrofloxacin, furazolidone and malachite green in fish products with surface-enhanced Raman spectroscopy. Food Chem 135: 845–850
30. Huo SH, Yan XP (2012) Metal-organic framework MIL-100(Fe) for the adsorption of malachite green from aqueous solution. J Mater Chem 22:7449–7455
31. Wang B, Zhang L, Zhou X (2014) Synthesis of silver nanocubes as a SERS substrate for the determination of pesticide paraoxon and thiram. Spectrochim Acta A 121:63–69